1-(2,4-Dibromophenyl)-3,6,6-trimethyl-1,5,6,7-tetrahydro-4*H*-indazol-4-one

A Novel Opioid Receptor Agonist with Less Accompanying Gastrointestinal Dysfunction than Morphine

Po-Kuan Chao, Ph.D., Shau-Hua Ueng, Ph.D., Li-Chin Ou, Ph.D., Teng-Kuang Yeh, Ph.D., Wan-Ting Chang, M.S., Hsiao-Fu Chang, M.S., Shu-Chun Chen, M.S., Pao-Luh Tao, Ph.D., Ping-Yee Law, Ph.D., Horace H. Loh, Ph.D., Ming-Fu Cheng, Ph.D., Jian-Ying Chuang, Ph.D., Chiung-Tong Chen, Ph.D., Chuan Shih, Ph.D., Shiu-Hwa Yeh, Ph.D.

ABSTRACT

Background: The authors investigated the pharmacology and signaling pathways of the opioid receptors modulated by compound 1, 1-(2,4-dibromophenyl)-3,6,6-trimethyl-1,5,6,7-tetrahydro-4*H*-indazol-4-one.

Methods: *In vitro* studies of compound 1 were assessed by using a radioligand-binding assay (n = 3), a cyclic adenosine monophosphate assay (n = 3), a β-arrestin assay (n = 3), an internalization assay (n = 3), and an immunohistochemistry (n = 8). *In vivo* studies of compound 1 were characterized using a tail-flick test (n = 5 to 6), tail-clip test (n = 7), von Frey hair test (n = 5), and charcoal meal test (n = 5).

Results: Compound 1 elicited robust effects in μ-opioid (mean ± SD; binding affinity: 15 ± 2 nM; cyclic adenosine monophosphate assay: 24 ± 6 nM), δ-opioid (82 ± 7 nM; 1.9 ± 0.1 μM), and κ-opioid (76 ± 9 nM; 1.4 ± 0.5 μM) receptor–expressing cells. Compound 1 acts as a full agonist of β-arrestin-2 recruitment in μ-opioid (1.1 ± 0.3 μM) and δ-opioid (9.7 ± 1.9 μM) receptor–expressing cells. Compound 1 caused less gastrointestinal dysfunction (charcoal meal test: morphine: 82 ± 5%; compound 1: 42 ± 5%) as well as better antinociception in mechanical pain hypersensitivity (tail-clip test: morphine: 10 ± 3 s; compound 1: 19 ± 1 s) and in cancer-induced pain (von Frey hair test: morphine: 0.1 ± 0.1 g; compound 1: 0.3 ± 0.1 g) than morphine at equi-antinociceptive doses.

Conclusions: Compound 1 produced antinociception with less gastrointestinal dysfunction than morphine. **(Anesthesiology 2017; 126:952-66)**

OPIOIDS are the most effective analgesics in clinical use for the alleviation of moderate to severe pain.[1] Among opioids, morphine is the mainstay of modern pain management.[2] Opioids and their analogs bind to opioid receptors of the G-protein–coupled receptor family, have site-specific effects, and are expressed mainly in the central nervous system.[3] Three subtypes of opioid receptors are present in the mammalian brain: the μ-opioid receptor, δ-opioid receptor, and κ-opioid receptor, and they result in inhibition of cyclic adenosine monophosphate (cAMP) production, β-arrestin recruitment, and activation of G-protein–coupled inwardly rectifying potassium channels.[4] μ-Opioid receptor is crucial to the analgesic and reward-related effects of opioids *in vivo* because the antinociceptive and rewarding effects of morphine are both eliminated in μ-opioid receptor knockout mice.[5]

What We Already Know about This Topic

- Opioid agonists are effective analgesics and exert their effects through μ-, δ-, or κ-opioid receptors. Currently used opioid agonists also cause unwanted side effects, including respiratory depression, sedation, constipation, and tolerance.
- Compound 1 was synthesized, structurally different from conventional opioids, and shown to be antinociceptive in mice.

What This Article Tells Us That Is New

- Compound 1 was further tested and found to be an agonist at μ-, δ-, and κ-opioid receptors but caused antinociception exclusively *via* μ-receptor activation.
- Compared with morphine, compound 1 caused greater antinociception but less gastrointestinal slowing.

Although opioids are effective drugs, they are also associated with a range of side effects, including tolerance, dependence, addiction, constipation, and respiratory

P.-K.C. and S.-H.U. contributed equally to this article.

Submitted for publication April 8, 2016. Accepted for publication January 17, 2017. From the Institute of Biotechnology and Pharmaceutical Research (P.-K.C., S.-H.U., L.-C.O., T.-K.Y., W.-T.C., H.-F.C., S.-C.C., M.-F.C., C.-T.C., C.S., S.-H.Y.) and Center for Neuropsychiatric Research (P.-L.T.), National Health Research Institutes, Zhunan, Taiwan; Department of Pharmacology, Medical School University of Minnesota, Minneapolis, Minnesota (P.-Y.L., H.H.L.); and the Ph.D. Program for Neural Regenerative Medicine, Taipei Medical University, Taipei, Taiwan (J.-Y.C., S.-H.Y.).

 Anesthesiology 2017; 126:952-66

<zdoi;10.1097/ALN.0000000000001568>

depression.[6–9] Most opioids are morphine-like compounds or morphine analogs, such as oxycodone, hydrocodone, and hydromorphone. Previous attempts to modify the structure of morphine-like opioids in order to diminish their side effects have failed. This may be because these analogs shared similar chemical structures, induced similar conformational changes in μ-opioid receptor, and activated the same signaling pathways as morphine. Therefore, high-throughput screening assays of compounds to discover new scaffolds of nonpeptide opioid receptor agonists may be an effective strategy for developing novel and effective analgesics that do not have severe adverse effects.

We have previously discovered a new opioid compound, 1-(2,4-dibromophenyl)-3,6,6-trimethyl-1,5,6,7-tetrahydro-4*H*-indazol-4-one (compound 1; fig. 1),[10] which has a novel chemical structure and exerts opioid receptor–dependent antinociception. In the current study, we examined the cellular signaling pathways activated by compound 1. We validated the pharmacologic effects of compound 1 in thermal and mechanical nociceptive tests and in animal models of cancer pain and gastrointestinal dysfunction in order to determine its efficacy and tolerability as compared to morphine. We also elucidated aspects of the mechanism of action of morphine and clarified areas for further improvements of such compounds.

Materials and Methods

Animals

Male wild-type C57BL/6 (B6) mice (25 to 30 g) and μ-opioid receptor knockout mice[5] (kindly provided by Dr. Tao) were kept in a temperature-controlled animal room with a 12-h:12-h light–dark cycle. The protocol was approved by the Institutional Animal Care and Use Committee of the National Health Research Institutes, Zhunan, Taiwan. Animal experiments were conducted in accordance with the Policies on the Use of Animals in Neuroscience Research and the ethical guidelines for investigations of experimental pain in conscious animals established by the International Association for the Study of Pain (Washington, D.C.). In each experiment, animals were randomized to an experimental group.

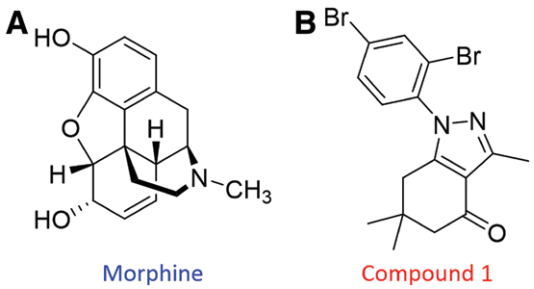

Fig. 1. Molecular structure of (*A*) morphine and (*B*) compound 1, 1-(2,4-dibromophenyl)-3,6,6-trimethyl-1,5,6,7-tetrahydro-4*H*-indazol-4-one.

Materials

Compound 1 was synthesized by Dr. Ueng. Morphine hydrochloride was obtained from the Food and Drug Administration, Ministry of Health and Welfare, Taipei, Taiwan. [Met5]Enkephalin was obtained from Sigma Chemical Co., USA. [^{3}H]Diprenorphine was obtained from PerkinElmer Inc., USA. [D-Pen2,D-Pen5]Enkephalin, *trans*-(–)-3,4-dichloro-*N*-methyl-*N*-[2-(1-pyrrolidinyl)cyclohexyl] benzeneacetamide hydrochloride, cyprodime, naltrindole, and nor-binaltorphimine were obtained from Tocris Biosciences, United Kingdom.

Radioligand Binding Assay

Human embryonic kidney 293 cells expressing human μ-opioid receptor, human δ-opioid receptor, and human κ-opioid receptor (provided by Dr. Law) were harvested and homogenized in membrane preparation buffer (50 mM Tris-HCl, pH 7.4, 2 mM EDTA) containing fresh protease inhibitor cocktail (Roche, Switzerland) and then centrifuged at 30,000*g* for 30 min. The pellets were resuspended, aliquoted, and stored at −80°C. For the [^{3}H]diprenorphine saturation binding assay, membranes (with 25 μg protein) were incubated with different concentrations (0.5 to 5 nM) of [^{3}H]diprenorphine in binding buffer (50 mM Tris-HCl, pH 7.4, 2 mM EDTA) at 25°C for 1 h. For competitive binding experiments, [^{3}H]diprenorphine (1 nM) was incubated with membranes (25 μg protein) in the absence or presence of various concentrations of compounds at 25°C for 1 h. Samples were then rapidly filtered onto glass-fiber filters (Millipore, USA) and washed three times with ice-cold phosphate-buffered saline. The radioactivity was quantified using a liquid scintillation counter.

Internalization Assay

The PathHunter G-protein–coupled receptor-internalization assay (DiscoveRx, USA) was performed according to the manufacturer's protocol. Briefly, human osteosarcoma U2OS cells express human μ-opioid receptor with complementary pieces of β-galactosidase that are genetically fused to the receptor and to a component of the endocytic vesicle. When activated, μ-opioid receptor interacts with the endosomes in this study, and the two fusion proteins form a complete enzyme whose activity can be detected by chemiluminescence. Cells were grown to confluence in McCoy's 5A medium (GIBCO, USA) containing 10% fetal bovine serum (FBS), 100 U/ml penicillin, 100 μg/ml streptomycin, 20 μg/ml G418 (Sigma Chemical Co.), 5 μg/ml hygromycin B (InvivoGen, USA), and 25 mM HEPES in T-175 tissue culture flasks (Corning, USA) and harvested with Cell Detachment Reagent (DiscoveRx). Cells (5,000 per well) were then seeded in black 384-well assay plates (Corning) with a CP5 reagent (DiscoveRx) and incubated for 24 h before the experiments. After each treatment, cells were incubated at room temperature for 1.5 h, followed by the addition of 8 μl PathHunter Detection reagent (DiscoveRx) and incubation for 1 h, and analyzed for chemiluminescence

on a Victor 2 plate reader (PerkinElmer Inc.). Experiments shown in each figure were performed on the same day, using the same generation of cells to ensure accurate comparisons of data.

β-Arrestin-2 Recruitment (β-Arrestin Assay)

The PathHunter G-protein–coupled receptor β-arrestin-2 assay (DiscoveRx) was performed according to the manufacturer's protocol. Briefly, when β-arrestin-2 translocates to the active receptor, complementary β-galactosidase fragments fuse to the receptor and β-arrestin-2 interacts to form a functional enzyme, which can be detected by chemiluminescence. Chinese hamster ovary cells expressing human μ-opioid receptor or human δ-opioid receptor were grown to confluence in F12 medium (GIBCO) containing 10% FBS, 100 U/ml penicillin, 100 μg/ml streptomycin, 200 μg/ml G418, and 20 μg/ml hygromycin B in T-175 tissue culture flasks (Corning) and harvested with Cell Detachment Reagent (DiscoveRx). Cells (5,000 per well) were then seeded in black 384-well assay plates (Corning) with a CP2 reagent (DiscoveRx) and incubated for 24 h before the experiments. Human osteosarcoma U2OS cells expressing κ-opioid receptor were grown to confluence in McCoy's 5A medium (GIBCO) containing 10% FBS, 100 U/ml penicillin, 100 μg/ml streptomycin, 20 μg/ml G418 (Sigma Chemical Co.), 5 μg/ml hygromycin B (InvivoGen), and 25 mM HEPES in T-175 tissue culture flasks (Corning) and harvested with a Cell Detachment Reagent (DiscoveRx). Cells (5,000 per well) were then seeded in black 384-well assay plates (Corning) with a CP5 reagent (DiscoveRx) and incubated for 24 h before the experiments. After each treatment, cells were incubated at room temperature for 1.5 h, followed by the addition of 8 μl PathHunter Detection reagent (DiscoveRx) and incubation for 1 h. Luminescence was detected using a Victor 2 plate reader (PerkinElmer Inc.). Experiments were performed on the same day, and the same passage of cells was used to ensure accurate comparisons of data.

cAMP Assay

Human embryonic kidney 293 cells expressing human μ-opioid receptor, human δ-opioid receptor, and human κ-opioid receptor were cultured in high-glucose Dulbecco modified Eagle medium (DMEM; GIBCO) supplemented with 10% FBS, 100 U/ml penicillin, 100 μg/ml streptomycin, 400 μg/ml G418, and 2 mM L-glutamine in T-175 tissue culture flasks (Corning) and harvested with trypsin–EDTA solution (GIBCO). Cells (72,000 per well) were plated in 100 μl/well DMEM in 96-well solid-bottom white plates (GIBCO) and 50 μl/well drug in Hanks balanced salt solution in the presence of forskolin and 3-isobutyl-1-methylxanthine at final concentrations of 1 and 500 μM, respectively. After 30 min of incubation at room temperature, the concentration of cAMP was determined using a LANCE Ultra cAMP Assay kit (PerkinElmer Inc.). Two hours later, plate fluorescence was measured using a Victor 2 plate reader (PerkinElmer Inc.) with excitation at 330 nm and emission at 615 and 665 nm.

Membrane Potential Assay

Mouse pituitary AtT-20 cells were cultured in DMEM containing 10% FBS, 100 U/ml penicillin, and 100 μg/ml streptomycin in T-175 tissue culture flasks (Corning) and harvested with a trypsin–EDTA solution. Cells (25,000 per well) were transiently transfected with myc-tagged human μ-opioid receptor plasmid (provided by Dr. Law, University of Minnesota) using NEPA21 electroporator gene transfection system (Nepa Gene, Japan) and subsequently seeded in black 96-well clear, flat-bottomed assay plates (Corning). The poring pulse conditions for electroporation were as follows: 110 V, 7.5-ms pulse length, 50-ms interpulse interval, and a 10% decay rate with plus polarity. The transfer pulse conditions were as follows: 20 V, 50-ms pulse length, 50-ms pulse interval, and a 40% decay rate with plus and minus polarities.[11] After 24 h, cells were serum starved for 3 h to detect potassium conductance changes using a fluorometric imaging plate reader (FLIPR; Molecular Devices, USA) membrane potential assay according to the manufacturer's instructions. Briefly, cells were treated with blue membrane potential dye for 0.5 h at 25°C. The fluorescence signal (excitation: 485 nm, emission: 525 nm) was monitored at intervals of 1.52 s, up to 150 s after the treatment on a FlexStation 3 bench-top multimode microplate reader (Molecular Devices).

Immunostaining

Mice were anesthetized with isoflurane, euthanized 1 h after the drug treatment, and perfused transcardially with 1× phosphate-buffered saline followed by 4% paraformaldehyde. The dorsal root ganglion was removed and postfixed for 12 h in 4% paraformaldehyde and then cryoprotected in 20% glycerol for 6 h at 4°C. The dorsal root ganglion sections were glued to the platform of a Vibroslice tissue slicer (DTK-1000; Dosaka, Japan). Transverse sections of 20-μm thickness were cut, and the appropriate slices from each group were placed on the same microscope slide and processed identically during a standard immunofluorescence staining procedure. The sections were first incubated with phosphate-buffered saline or wheat germ agglutinin conjugated with Alexa488 (1:1,000; Cat. W11261; Molecular Probes, USA) to label the plasma membrane. After washing, the sections were incubated with permeabilization buffer (0.4% Triton X-100 and 2% FBS in phosphate-buffered saline) for 1 h and then in phosphate-buffered saline with rabbit monoclonal anti–β-arrestin-2 antibody (1:1,000; Cat. AB6022; Millipore) or rabbit monoclonal anti-μ-opioid receptor antibody (1:500; Cat. NBP1-96656; Novus Biologicals, USA) for 24 h. Subsequently, the sections were washed four times with the washing buffer (0.2% Triton X-100 in phosphate-buffered saline) and then incubated in phosphate-buffered

saline with Alexa488-conjugated goat anti-rabbit immunoglobulin G antibody (1:1,000; Cat. A-11034; Invitrogen, USA), Alexa568-conjugated goat anti-rabbit immunoglobulin G antibody (1:1,000; Cat. A-11036; Invitrogen), or 4',6-diamidino-2-phenylindole for 1 h. The slides were then washed three times with phosphate-buffered saline and mounted with glycerol. Fluorescence images were captured using a laser confocal microscope (TCS SP5II; Leica, Germany) and acquired using the same gain and exposure time. The number of puncta representing the β-arrestin-2 (diameter greater than 0.3 μm) and cytoplasmic μ-opioid receptor per cell were measured from confocal images of eight randomly selected fields per experiment using ImageJ (National Institutes of Health, USA) with qualifications.[12]

Tail-flick Test

Drug-induced antinociception against acute thermal pain hypersensitivity was evaluated using the Tail-Flick Analgesia Meter (Columbia Instruments, USA). Mice with a basal latency between 2.5 and 3 s were collected and randomly divided into each group. The basal latency was recorded before treatment, and tail-flick latencies were recorded 30, 60, 90, 120, and 180 min after iv, intraperitoneal, or intrathecal administration of drugs. Morphine and naloxone were dissolved in saline. The iv dosing solution of compound 1 was prepared in 5% dimethyl sulfoxide, 5% cremophor, and 90% saline. Cyprodime, naltrindole, and nor-binaltorphimine were prepared in 5% dimethyl sulfoxide and 95% saline. A cutoff time of 10 s was set to avoid tissue damage. The antinociceptive effect was defined as the difference between the tail-flick latency and the basal latency at each time point. The area under the curve (AUC) value was obtained by calculating the area under the time–response curve of the antinociceptive effect after treatment of the drugs. The percentage of the maximum possible effect was calculated as [(tail-flick latency – basal latency) ÷ (cutoff time – basal latency)] × 100.[13]

Tail-clip Test

Each mouse was placed in an acrylic box (10 cm in diameter, 30 cm in height) and allowed to acclimate for 5 min before testing, and then a clip was applied 1 cm from the base of the tail. The latency to bite or grasp the clip was measured while the clip was being applied to the tail.[14] Regardless of the response, a cutoff time of 20 s was set to avoid tissue damage.

Cancer-induced Pain and Mechanical Allodynia Test

Mouse B16-F1 melanoma cells were cultured in DMEM containing 10% FBS, 100 U/ml penicillin, and 100 μg/ml streptomycin in T-175 tissue culture flasks (Corning) and harvested with trypsin–EDTA solution. To induce cancer pain, each B6 mouse was injected with either 20 μl phosphate-buffered saline or cells (6×10^5 cells/20 μl phosphate-buffered saline) in the footpad of the right hind paw under isoflurane anesthesia on postinoculation day 0. On postinoculation day 19, the test day, mice were placed on a mesh floor with 5- × 5-mm holes, covered with a cup to prevent visual stimulation, and allowed to adapt for 1 h before testing. Melanoma cell–injected mice were intravenously administered vehicle, morphine, or compound 1, and 50% withdrawal threshold was subsequently evaluated using a classical up-and-down method with von Frey filaments (range, 0.1 to 1 g; IITC Life Science, USA).[15] Testing was initiated with 0.5 *g* force. Briefly, whenever a withdrawal response occurred, the next weaker von Frey filament was applied; however, whenever no withdrawal response occurred, the next stronger filament was applied. Mechanical allodynia was defined as changes in the amount of pressure required to induce withdrawal.

Charcoal Meal Test

Briefly, B6 mice were fasted for at least 16 h before the experiments with free access to water. Various doses of drugs were administered to the mice 15 min before the administration of an aqueous activated charcoal suspension (10% activated charcoal plus 5% gum Arabic; 0.3 ml). After 30 min, the mice were euthanized by intraperitoneal administration of a ketamine–xylazine cocktail (Sigma Chemical Co.) followed by cervical dislocation, and the total length of migration of the charcoal meal was measured from the pylorus to the ileocecal junction of the small intestine. Gastrointestinal propulsion was calculated as the percentage of the distance traveled by the charcoal meal relative to the total length of the small intestine to control for individual variations. A gastrointestinal propulsion rate of less than 55% indicated a clear inhibition of bowel propulsion.

Statistical Analysis

All *in vitro* and *in vivo* experiments were repeated multiple times as indicated in the figure legends to ensure the reliability of the individual values. The sample size used in all experiments was based on previous experience. No samples, mice, or data points were excluded from the reported analysis. Investigators were blinded to the test conditions. In all experiments, an individual administered drugs to the cells or animals, and another individual who was blinded to the drug administered observed the response and analyzed the data. Data are presented as individual data points or as mean ± SD (GraphPad Prism version 5.00 for Windows; GraphPad Software, USA). Opioid receptor-binding affinity (*Ki*; table 1), EC_{50} (table 2), or curve fits of dose–response curves (figs. 2–4) of each compound were determined using a nonlinear regression analysis. In the *in vivo* experiments, three types of statistical analyses were performed. For the time–response curves of vehicle, morphine, or compound 1 (figs. 5–7), a two-way ANOVA with a Bonferroni *post hoc* test was used. For the quantitative results from the time–response curves (figs. 5 and 6), the distribution of β-arrestin-2 and μ-opioid receptor (fig. 3), or the 30-min treatment experiment to investigate the antinociception or gastrointestinal inhibition produced by the compounds (figs. 4 and

Table 1. Opioid Receptor-binding Affinity of Morphine and Compound 1 on μ-Opioid Receptor, δ-Opioid Receptor, and κ-Opioid Receptor

	[^{3}H]Diprenorphine Binding, *K*i		
	MOR	DOR	KOR
Morphine, nM	6.8 ± 0.8	55 ± 8	25 ± 3
Compound 1, nM	15 ± 2	82 ± 7	76 ± 9
ME, nM	1.5 ± 0.3	ND	ND
DPDPE, nM	ND	2.3 ± 0.5	ND
U50488, nM	ND	ND	3.1 ± 1.2

Receptor-binding affinities were measured by competitive inhibition of [^{3}H] diprenorphine-binding assessment performed by using MOR, DOR, and KOR membranes. *K*i = half-maximal inhibitory concentration/(1 + *L*/*K*d), where *L* is the concentration of [^{3}H]diprenorphine used (1 nM), and the *K*d values in MOR, DOR, and KOR are 0.46, 0.65, and 0.33 nM, respectively. All experiments were carried out independently and at least in triplicate. The values indicate the mean ± SD.

DOR = δ-opioid receptor; DPDPE = [D-Pen2,D-Pen5]enkephalin; *K*i = opioid receptor-binding affinity; KOR = κ-opioid receptor; ME = [Met5] enkephalin; MOR = μ-opioid receptor; ND = not determined; U50488 = *trans*-(–)-3,4-dichloro-*N*-methyl-*N*-[2-(1-pyrrolidinyl)cyclohexyl]benzeneacetamide hydrochloride.

5), a one-way ANOVA with Newman–Keuls *post hoc* tests was used. For the comparison of maximum possible effect (Emax) values between morphine and compound 1 (fig. 4) or the comparison of the mechanical allodynia between sham-control and melanoma cell–implanted mice (fig. 7), a Student's *t* test was used. $P < 0.05$ was considered statistically significant.

Results

Opioid Receptor Signaling Pathways Are Regulated by Compound 1

Previously, we had identified a series of chemical compounds for human μ-opioid receptor activation and further optimized them for potency and selectivity, resulting in the discovery of compound 1, which had the lowest opioid receptor-binding affinity as well as the best *in vivo* antinociception activity among the compounds in the series.[10] Compound 1 has no structural similarity to any other previously described μ-opioid receptor agonist, and we conducted these experiments to determine, in part, the effects of compound 1 on μ-opioid (fig. 2) and δ- and κ-opioid (fig. 3) receptor–mediated signaling pathways.

First, we performed competitive receptor-binding assays in μ-opioid receptor, δ-opioid receptor, and κ-opioid receptor membranes to determine the binding affinity of morphine and compound 1, using a nonselective opioid ligand tracer [^{3}H]diprenorphine. Both morphine and compound 1 have the highest affinity for μ-opioid receptor, followed by κ-opioid receptor and δ-opioid receptor (table 1). The binding affinity of compound 1 for μ-opioid receptor, δ-opioid receptor, and κ-opioid receptor was 2.2-, 1.5-, and 3-fold less than that of morphine, respectively (table 1). To test the agonist property of compounds, compound 1 and morphine were subjected to cAMP assays in μ-opioid receptor–expressing cells, as they reflect the G-protein–dependent signaling pathway activated by μ-opioid receptor. Both compound 1 and morphine significantly decreased cAMP production in μ-opioid receptor–expressing cells in a dose-dependent manner (fig. 2A); the potency of compound 1 was higher than that of morphine (table 2). Furthermore, the Emax of compound 1 on cAMP inhibition, observed at 10 to 100 μM, was 1.4 times higher than that of the morphine group (fig. 2A). Moreover, compound 1 also activated G protein pathways in δ-opioid receptor–expressing cells (fig. 3A) and κ-opioid receptor–expressing cells (fig. 3B), and its Emax was comparable with those of [D-Pen2,D-Pen5]enkephalin (a δ-opioid receptor agonist) and *trans*-(–)-3,4-dichloro-*N*-methyl-*N*-[2-(1-pyrrolidinyl)cyclohexyl]benzeneacetamide hydrochloride (a κ-opioid receptor agonist).

Next, we determined whether compound 1 had any effect on the G-protein–coupled inwardly rectifying potassium channel activation, as this is another μ-opioid receptor G-protein–dependent signaling pathway that contributes to opioid receptor–mediated analgesia.[16] The pituitary AtT-20 cells, which highly express the endogenous G-protein–coupled inwardly rectifying potassium channel, are a suitable cellular model for conducting a potassium channel assay.[17] Acute treatment with morphine caused a μ-opioid receptor–dependent membrane potential hyperpolarization in myc-tagged

Table 2. The EC_{50} of Morphine and Compound 1 in the Functional Cell-based Assays Presented in Figures 2 and 3

	cAMP			β-Arrestin-2			MOR Internalization	Membrane Potential
	MOR	DOR	KOR	MOR	DOR	KOR	MOR	MOR
Morphine	42 ± 4 nM	ND	ND	0.6 ± 0.1 μM	0.8 ± 0.2 μM	4.5 ± 2.6 μM	0.8 ± 0.2 μM	34 ± 1 nM
Compound 1	24 ± 6 nM	1.9 ± 0.1 μM	1.4 ± 0.5 μM	1.1 ± 0.3 μM	9.7 ± 1.9 μM	29 ± 10 μM	12 ± 5 μM	6.1 ± 1.6 μM
ME	ND	ND	ND	26 ± 1 nM	ND	ND	100 ± 20 nM	ND
DPDPE	ND	1.6 ± 0.1 nM	ND	ND	17 ± 3 nM	ND	ND	ND
U50488	ND	ND	1.9 ± 0.8 nM	ND	ND	0.6 ± 0.5 μM	ND	ND

All experiments were carried out independently and at least in triplicate. The values indicate the mean ± SD.

cAMP = cyclic adenosine monophosphate; DOR = δ-opioid receptor; DPDPE = [D-Pen2,D-Pen5]enkephalin; KOR = κ-opioid receptor; ME = [Met5] enkephalin; MOR = μ-opioid receptor; ND = not determined; U50488 = *trans*-(–)-3,4-dichloro-*N*-methyl-*N*-[2-(1-pyrrolidinyl)cyclohexyl]benzeneacetamide hydrochloride.

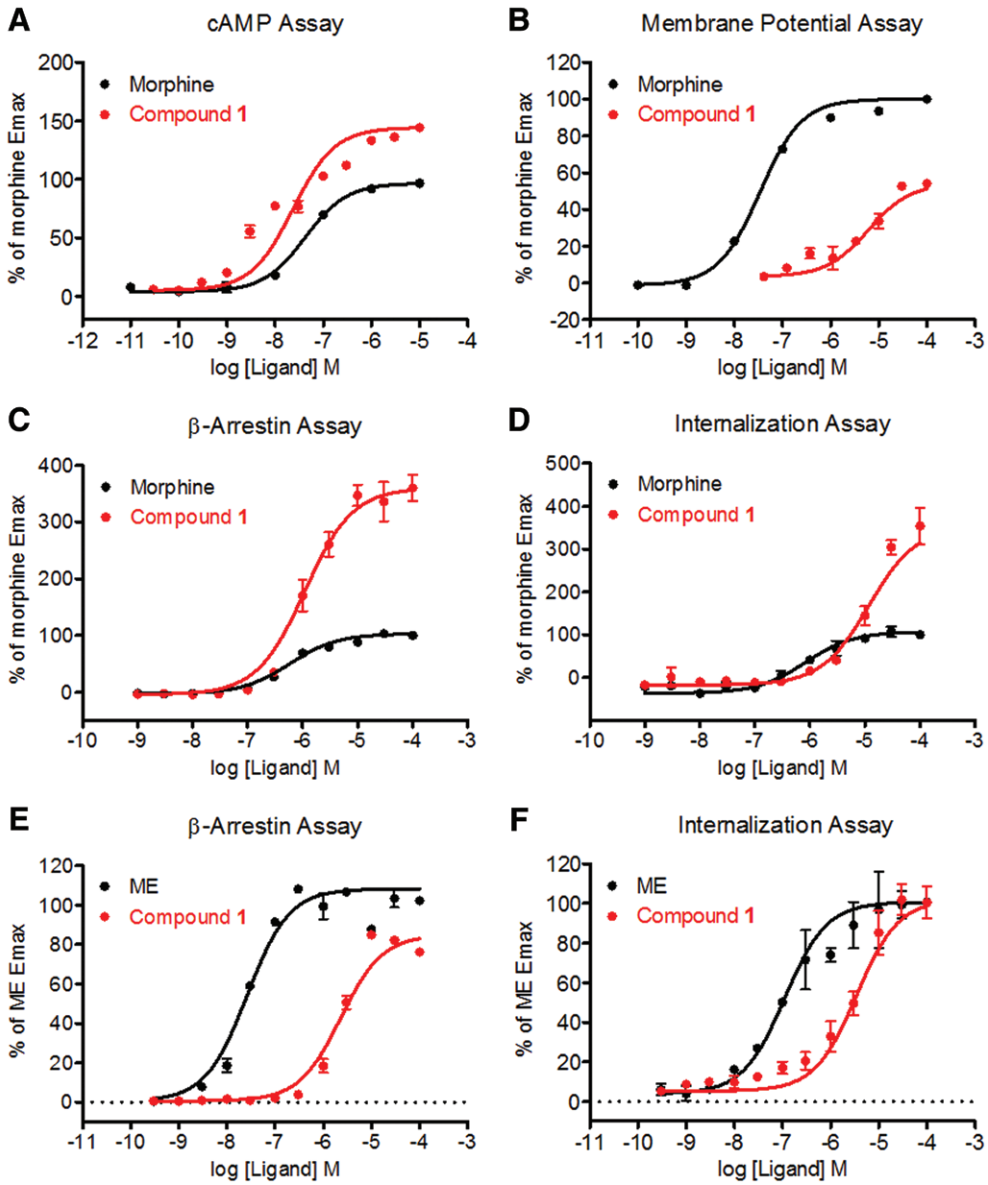

Fig. 2. Signaling pathways of μ-opioid receptor regulated by compound 1. (*A*) Compound 1 has a similar G-protein–coupling efficacy to morphine. G protein coupling was measured by the inhibition of cyclic adenosine monophosphate (cAMP) accumulation in human embryonic kidney 293 cells expressing human μ-opioid receptor (n = 3). (*B*) The effects of compound 1 and morphine on the activation of G-protein–coupled inwardly rectifying potassium channels. AtT-20 cells were transfected with a myc-tagged μ-opioid receptor expression plasmid before membrane potential assay (n = 3). (*C*, *E*) Treatment with compound 1 induces more β-arrestin-2 recruitment than morphine (*C*), with an effect similar to that of [Met5]enkephalin (*E*). β-Arrestin-2 recruitment was measured using the PathHunter enzyme complementation assay in Chinese hamster ovary cells expressing human μ-opioid receptor. Data in *C*, *E*, n = 3 per group. (*D*, *F*) Compound 1 induces more μ-opioid receptor endocytosis than morphine (*D*). Maximum possible effect (Emax) of compound 1- and [Met5]enkephalin-induced μ-opioid receptor endocytosis are similar (*F*). μ-Opioid receptor internalization was measured by an enzyme complementation assay in human osteosarcoma U2OS cells expressing human μ-opioid receptor. Data in *D*, *F*, n = 3 per group. ME = [Met5]enkephalin.

μ-opioid receptor–expressing AtT-20 cells. The Emax of compound 1 (100 μM), however, had only approximately 60% of the efficacy of morphine in the membrane potential assay (fig. 2B), and the EC_{50} of compound 1 was markedly higher than that of morphine (table 2). These results indicate that compound 1 failed to activate G-protein–coupled inwardly rectifying potassium channels or alter membrane potentials in μ-opioid receptor–expressing AtT-20 cells.

On the other hand, compound 1 treatment induced β-arrestin-2 recruitment, a G-protein–independent pathway, to μ-opioid receptor (fig. 2C) and δ-opioid receptor (fig. 3C) but not to κ-opioid receptor (fig. 3D). Compound 1 had a significantly higher Emax than morphine (fig.

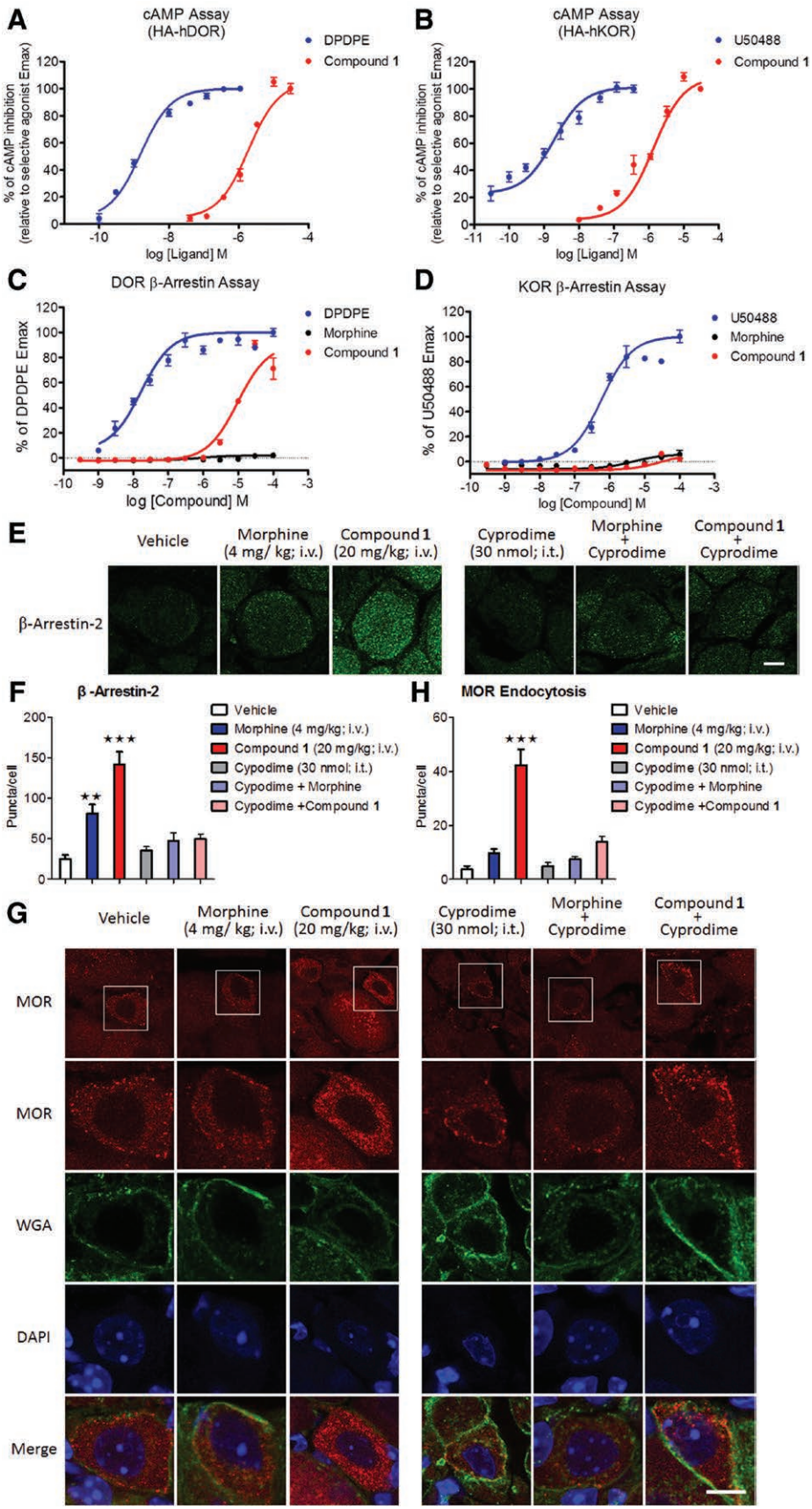

Fig. 3. *(Continued)*

Fig. 3. *(Continued).* Receptor subtype selectivity of compound 1. (*A*, *B*) No receptor subtype selectivity for compound 1 is noted between δ-opioid receptor (DOR) and κ-opioid receptor (KOR). The concentration–response curve of compound 1 in human embryonic kidney 293 cells expressing human DOR or KOR was measured by cyclic adenosine monophosphate production (cAMP) assay. The maximum possible effect (Emax) of compound 1-, [D-Pen2,D-Pen5]enkephalin-, and *trans*-(–)-3,4-dichloro-*N*-methyl-*N*-[2-(1-pyrrolidinyl)cyclohexyl]benzeneacetamide hydrochloride (U50488)–induced inhibition of cAMP accumulation are similar. Data in *A* and *B* are based on n = 3 per group. (*C*, *D*) β-Arrestin-2 recruitment was measured using the PathHunter enzyme complementation assay in Chinese hamster ovary cells expressing human DOR (*C*) and human osteosarcoma U2OS cells expressing human KOR (*D*). Data are displayed as the percentage of the maximum (*C*) [D-Pen2,D-Pen5]enkephalin (DPDPE) and (*D*) *trans*-(–)-3,4-dichloro-*N*-methyl-*N*-[2-(1-pyrrolidinyl)cyclohexyl]benzeneacetamide hydrochloride (U50488) efficacy to control for individual variations. Data in *C* and *D* are based on n = 3 per group. (*E–H*) Representative immunofluorescence images and quantification of the distribution of (*E*, *F*) β-arrestin-2 and (*G*, *H*) cytoplasmic μ-opioid receptor (MOR) in the mouse dorsal root ganglion after drug treatment. Mice were injected intrathecally with either vehicle or cyprodime 5 min before vehicle, morphine, or compound 1 injection, and 1 h later, samples were assessed by confocal microscopy. Wheat germ agglutinin (WGA) was used as a plasma membrane marker. 4',6-diamidino-2-phenylindole (DAPI) (*blue*) was used as a nuclear marker. *Scale bar* = 10 μm. **P* < 0.001 *versus* vehicle group, one-way ANOVA with appropriate *post hoc* tests. All values in *F* and *H* indicate the mean ± SD. Data in *E–H* are based on n = 8 per group.

2C; μ-opioid receptor: 3-fold; fig. 3B; δ-opioid receptor: 20-fold), even though the EC_{50} of compound 1 and morphine were similar in the β-arrestin assay (table 2). Furthermore, G-protein–coupled receptor internalization and desensitization occur after β-arrestin-2 recruitment.[18] Compound 1 induced significant μ-opioid receptor internalization in the μ-opioid receptor-internalization assay (fig. 2D), and the Emax of compound 1 was threefold higher than that of morphine, a poor μ-opioid receptor-internalizing opioid (fig. 2D), even though the EC_{50} of compound 1 was higher than that of morphine (table 2). Moreover, the Emax of compound 1, [Met5]enkephalin (μ-opioid receptor agonist; fig. 2E), and [D-Pen2,D-Pen5]enkephalin (δ-opioid receptor agonist; fig. 3C) were similar in β-arrestin-2 assays and μ-opioid receptor-internalization assays (fig. 2F). Finally, compound 1 induced significant μ-opioid receptor–dependent β-arrestin-2 recruitment (fig. 3, E and F; $F_{5,42} = 30.5$; $P < 0.001$; one-way ANOVA) and μ-opioid receptor endocytosis (fig. 3, G and H; $F_{5,42} = 33.1$; $P < 0.001$; one-way ANOVA) in dorsal root ganglion neurons *in vivo*, whereas both these effects were blocked by pretreatment of mice with cyprodime (a μ-opioid receptor–selective antagonist).

Constipation-inducing Properties of Morphine and Compound 1

The constipating potency of compound 1 relative to morphine was investigated using the charcoal meal test in order to assess its effects on gastrointestinal motility. As shown in figure 4, A and B, single iv doses of both compound 1 and morphine inhibited gastrointestinal transit of a charcoal meal. However, the ED_{50} of gastrointestinal transit (0.8 ± 0.5 mg/kg) was markedly lower than the ED_{50} of antinociception (1.9 ± 0.5 mg/kg) in the morphine-treated group (fig. 4A). In contrast, the ED_{50} of gastrointestinal transit (11 ± 1.7 mg/kg) and antinociception (11 ± 1.6 mg/kg) of compound 1 were similar (fig. 4B). Furthermore, compound 1 and morphine both produced a similar degree of antinociception at the maximal antinociceptive doses (fig. 4C; $P > 0.05$; Student's *t* test), whereas single (fig. 4D; $P < 0.001$; Student's *t* test) and repeated (fig. 4E; $P < 0.05$; Student's *t* test) compound 1 administration caused less gastrointestinal dysfunction than morphine at equi-antinociceptive doses. Thus, use of compound 1 as an analgesic may cause less constipation than morphine.

To determine whether compound 1–mediated gastrointestinal dysfunction was dependent on opioid receptor activation, mice were injected with either the vehicle or an opioid antagonist (naloxone, 10 mg/kg, intraperitoneal) before morphine (4 mg/kg, iv) or compound 1 (20 mg/kg, iv) injection, and the gastrointestinal motility of each compound was evaluated. Naloxone attenuated both the gastrointestinal dysfunction and antinociception (fig. 4F; $F_{4,20} = 21.8$; $P < 0.001$; fig. 4G; $F_{4,20} = 42.5$; $P < 0.001$; one-way ANOVA) produced by morphine and compound 1. Furthermore, no significant differences in gastrointestinal dysfunction and antinociception were observed among the vehicle-, morphine-, and compound 1–treated groups in the μ-opioid receptor knockout mice (fig. 4H; $F_{2,15} = 0.3$; $P > 0.05$; fig. 4I; $F_{2,15} = 0.4$; $P > 0.05$; one-way ANOVA). Thus, these findings suggest that the effects of morphine and compound 1 on gastrointestinal inhibition and antinociception were mediated through μ-opioid receptor signaling.

Compound 1 Produces Antinociceptive Effects in Mice

To further assess the effect of compound 1 on antinociception, nociceptive tests using thermal (fig. 5A–D) or mechanical (fig. 5E) stimuli were performed after acute drug treatments. Both acute morphine and compound 1 resulted in antinociception in a dose-dependent manner. However, the ED_{50} of compound 1 was weaker than that of morphine (fig. 4, A and B). The brain or plasma concentration measurement revealed that compound 1 was distributed throughout both the plasma and brain tissue 5 min after the iv injection; however, it had degraded significantly by 1 h later (table 3). Furthermore, morphine produced antinociceptive effects at doses of 1 to 4 mg/kg (fig. 5A; treatment $F_{3,16} = 26.7$, minute [min] $F_{5,80} = 28.2$, interaction $F_{15,80} = 6.8$; all $P < 0.001$; two-way ANOVA). Quantitative results from time–response curves were presented as the AUC, which revealed significant differences between the vehicle control and morphine-treated groups (fig. 5B; $F_{3,16} = 26.2$; $P < 0.001$; one-way ANOVA). Compound 1 produced similar antinociceptive effects in the equi-antinociceptive

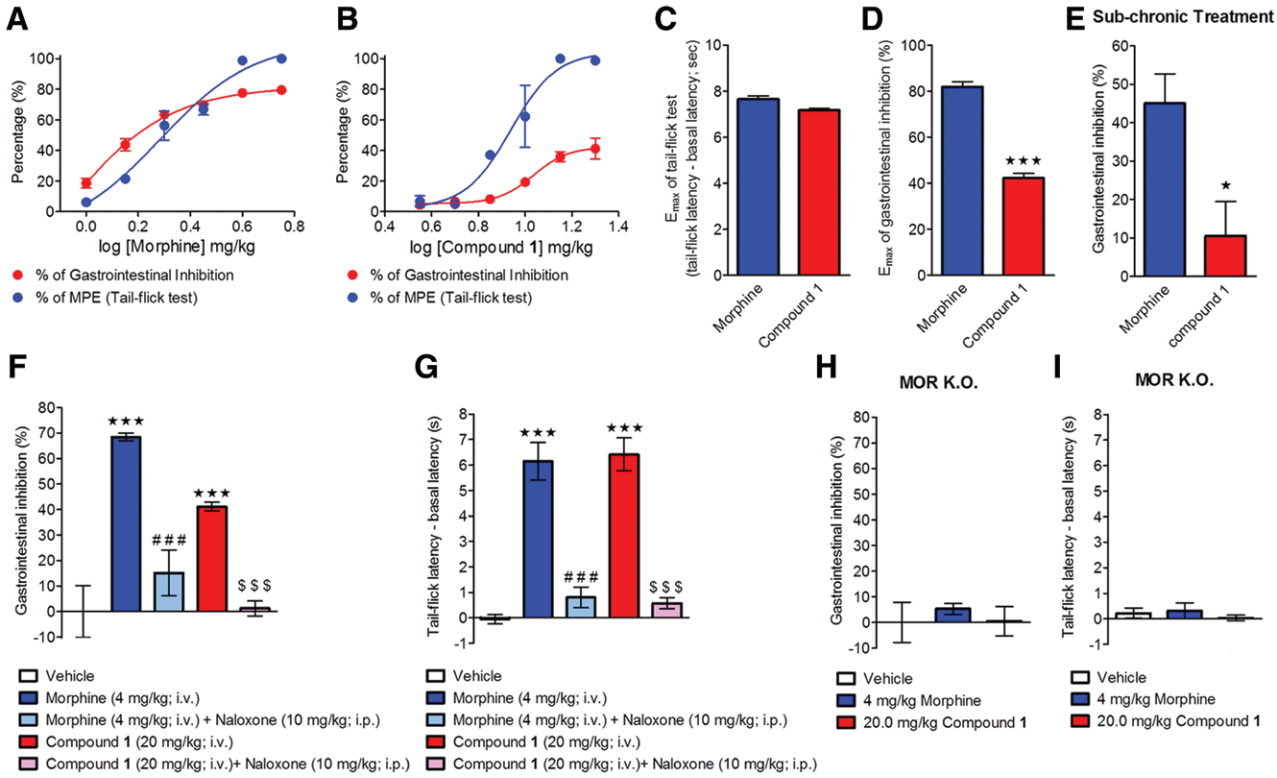

Fig. 4. Compound 1 causes less gastrointestinal dysfunction than morphine in mice. (*A*, *B*) Mice were intravenously injected with either morphine (*A*) or compound 1 (*B*) at the indicated doses and 30 min later were subjected to either a tail-flick test (*blue curves*) or a charcoal meal test (*red curves*). The antinociceptive effect of each drug was determined as the percentage of maximum possible effect (MPE), and the inhibition of gastrointestinal propulsion was calculated as the percentage of the distance traveled by the charcoal meal relative to the total length of the small intestine. Data in *A* and *B* are based on n = 5 per group. (*C*, *D*) Quantitative results from *A* and *B* are represented as the maximum possible effect (Emax) values. **P* < 0.001 *versus* morphine group, Student's *t* test. Data in *C* and *D* are based on n = 5 per group. (*E*) Mice were subchronically injected with morphine (4 mg/kg) or compound 1 (20 mg/kg) twice daily for 5 days and then were subjected to a charcoal meal test after the last injection. †*P* < 0.05 *versus* morphine group, Student's *t* test. n = 5 per group. (*F–I*) The experiments carried out in *F* and *G* were performed in wild-type mice, while those in *H* and *I* were performed in μ-opioid receptor knockout (MOR-KO) mice. Mice were injected with each treatment and 30 min later were subjected to either a charcoal meal test (*F*, *H*) or a tail-flick test (*G*, *I*). **P* < 0.001 *versus* vehicle group. ‡*P* < 0.001 *versus* morphine group. §*P* < 0.001 *versus* compound 1 group, one-way ANOVA with appropriate *post hoc* tests. Data in *F–I* are based on n = 5 to 6 per group. The values indicate the mean ± SD.

doses of 10 to 20 mg/kg (fig. 5C; treatment $F_{3,16}$ = 53.4, min $F_{5,80}$ = 39.5, interaction $F_{15,80}$ = 15.6; all P < 0.001; two-way ANOVA). Quantitative results from time–response curves revealed significant differences between the vehicle control and compound 1–treated groups (fig. 5D; $F_{3,16}$ = 100.8; P < 0.001; one-way ANOVA). Maximum antinociception for compound 1 was sustained up to 60 min after the injection. Moreover, both morphine and compound 1 reduced the pain sensitivity to the tail clip, further confirming the antinociceptive effect of compound 1 in acute mechanical pain hypersensitivity (fig. 5E; $F_{2,18}$ = 23; P < 0.001; one-way ANOVA). Finally, the antinociceptive effects of both morphine and compound 1 were blocked by pretreating mice with a μ-opioid receptor–selective antagonist but not with a δ-opioid or κ-opioid receptor–selective antagonist, indicating the μ-opioid receptor–dependent antinociception of morphine and compound 1 (fig. 5F; $F_{11,48}$ = 168; P < 0.001; one-way ANOVA).

After 5 days of twice-daily treatment, both equi-antinociceptive doses of morphine and compound 1 produced antinociceptive tolerance. Surprisingly, antinociceptive effects produced in the morphine group decreased more significantly than that in the compound 1 group (fig. 6A; treatment $F_{2,12}$ = 166.2, min $F_{5,60}$ = 192.8, interaction $F_{10,60}$ = 42.5; all P < 0.001; two-way ANOVA). We further investigated whether there was cross-tolerance between compound 1 and morphine, since they both activated μ-opioid receptor, despite their different chemical structures (fig. 1). Tail-flick tests were performed for compound 1 after subchronic treatments (twice daily for 5 days) with vehicle or morphine, as shown in figure 6B. The antinociceptive effect of compound 1 was decreased after subchronic morphine treatment, as compared to its efficacy before treatment. The magnitude of compound 1 in time–response curves indicated significant differences between the groups (fig. 6C; treatment

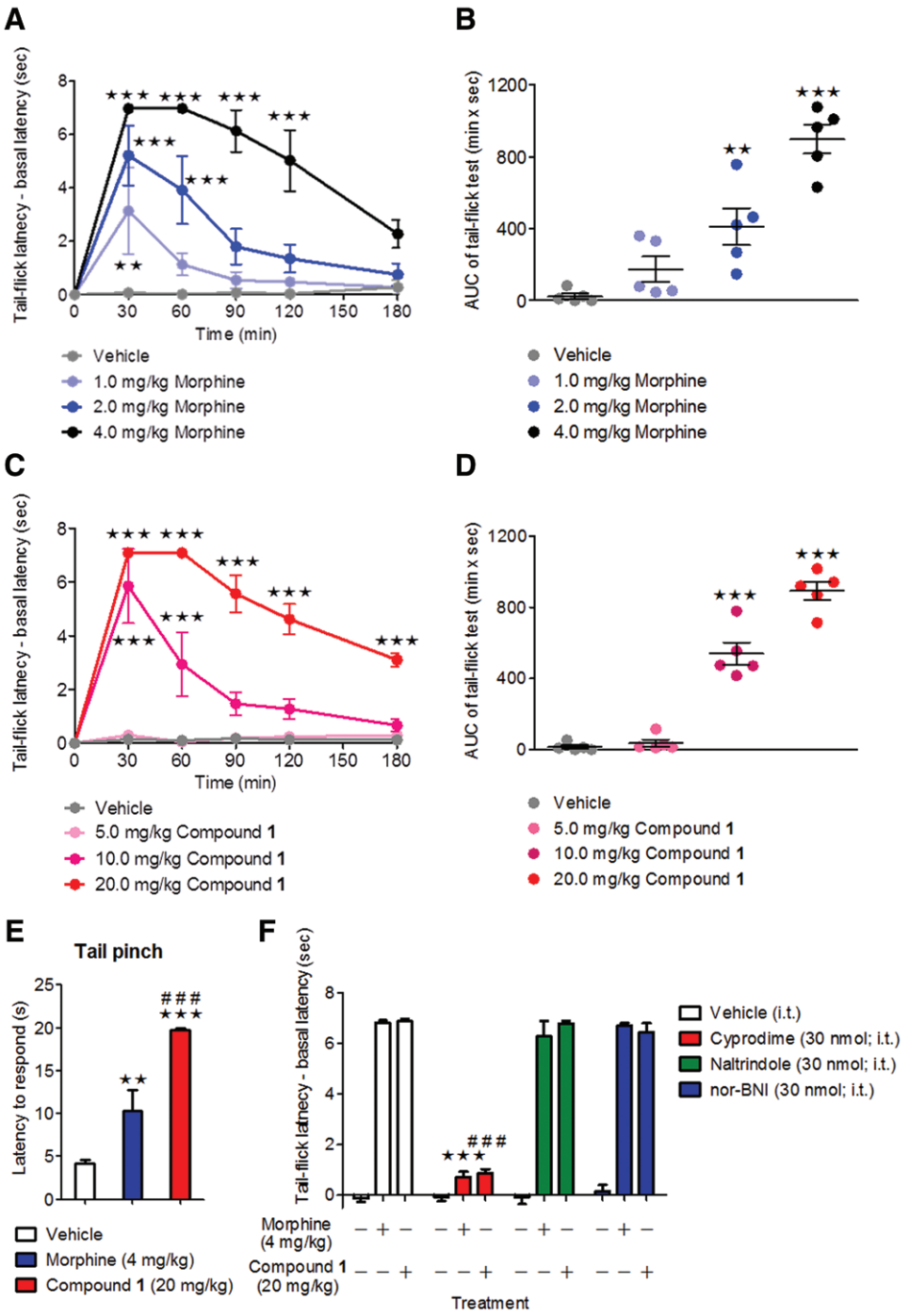

Fig. 5. Antinociceptive effects of morphine and compound 1 in wild-type C57BL/6 (B6) mice. (*A*, *C*) Acute antinociceptive effects of morphine (*A*) and compound 1 (*C*) in B6 mice. After detection of basal latencies, each mouse was injected with various dosages of either morphine or compound 1 to detect the radiant heat tail-flick latencies at the indicated time points (30, 60, 90, 120, 150, and 180 min after drug injection), and quantitative results were calculated. **P* < 0.01. †*P* < 0.001 *versus* vehicle group, two-way ANOVA with appropriate *post hoc* tests. Data in *A* and *C* are based on n = 5 per group. (*B*, *D*) Quantitative results from *A* and *C* are represented as the area under the curve (AUC). **P* < 0.01. †*P* < 0.001 *versus* vehicle group, one-way ANOVA with appropriate *post hoc* tests. Data in *B* and *D* are based on n = 5 per group. (*E*) Mice were injected with vehicle, morphine (4 mg/kg), or compound 1 (20 mg/kg), and then the acute mechanical pain sensitivity to a tail clip was measured. **P* < 0.01. †*P* < 0.001 *versus* vehicle group. ‡*P* < 0.01 *versus* morphine group, one-way ANOVA with appropriate *post hoc* tests. n = 7 per group. (*F*) Mice were injected intrathecally with cyprodime, naltrindole, or nor-binaltorphimine (nor-BNI) 5 min before vehicle, morphine (4 mg/kg), or compound 1 (20 mg/kg) injection and were subjected to a tail-flick test 30 min later. †*P* < 0.001 *versus* vehicle or morphine group. §*P* < 0.001 *versus* vehicle or compound 1 group, one-way ANOVA with appropriate *post hoc* tests. n = 5 per group. The values indicate the mean ± SD.

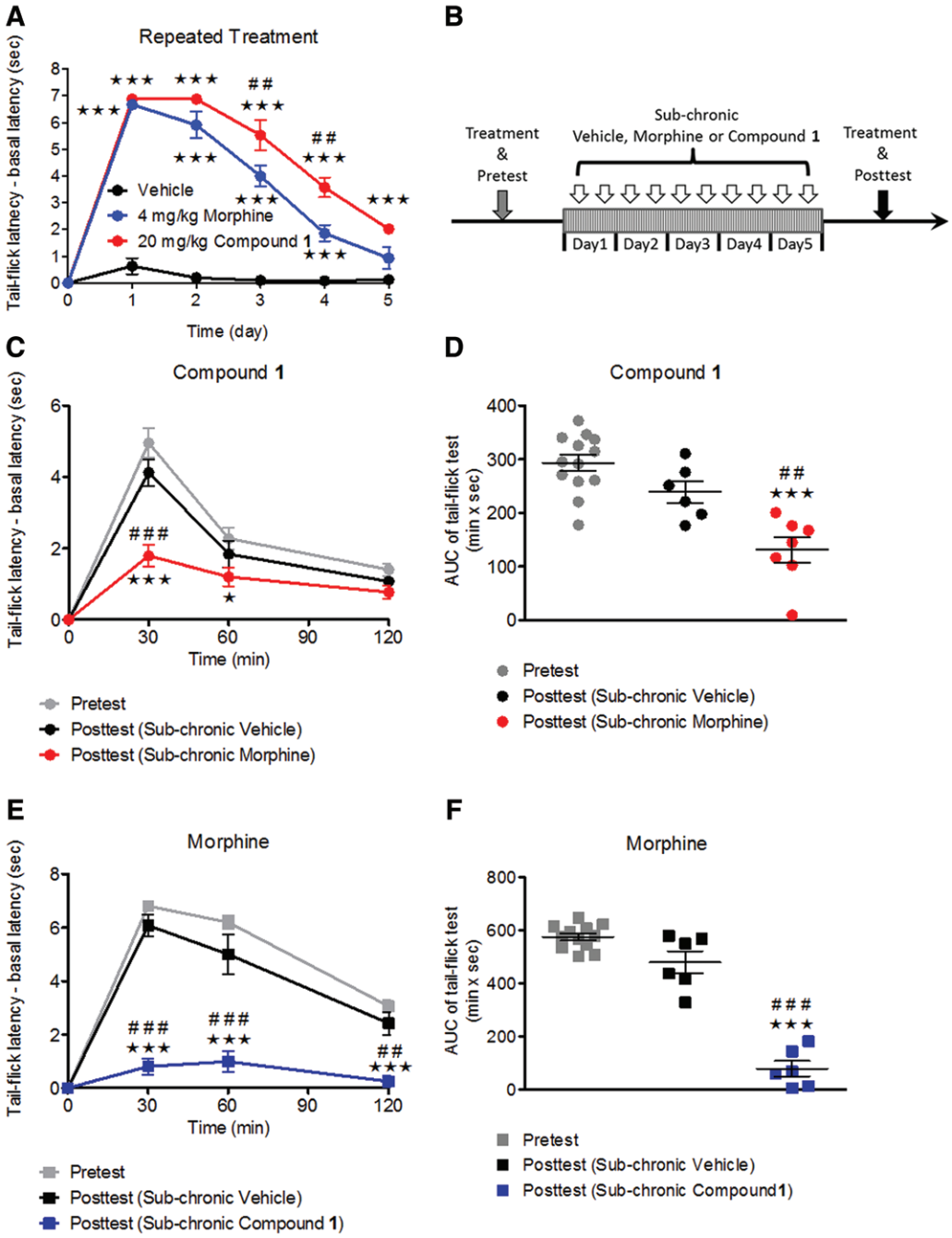

Fig. 6. Cross-tolerance between morphine and compound 1. (*A*) Subchronic antinociceptive effects of morphine and compound 1 in wild-type C57BL/6 mice. Mice in each group were first treated with vehicle on day 0 and were then subchronically injected with equi-antinociceptive doses of morphine (4 mg/kg) or compound 1 (20 mg/kg) twice daily for 5 days. The antinociceptive effect of each treatment was determined by testing the radiant heat tail-flick latency on days 0, 1, 2, 3, 4, and 5. **P* < 0.001 *versus* vehicle group. †*P* < 0.01 *versus* morphine group, two-way ANOVA with appropriate *post hoc* tests. n = 5 per group. (*B*) The flowchart of the experiments used to test the cross-tolerance effects of morphine and compound 1. The time–response curve of acute morphine (4 mg/kg) or compound 1 (20 mg/kg) was determined by testing the radiant heat tail-flick latency before the chronic treatment of vehicle, morphine, or compound 1. For subchronic treatment, mice were then injected intravenously with vehicle or drugs (morphine: 10 mg/kg; compound 1: 20 mg/kg; twice daily for 5 days) to generate morphine- or compound 1–tolerant mice, and time–response curves of morphine (4 mg/kg) or compound 1 (20 mg/kg) were then determined once more. (*C*, *E*) The antinociceptive effects of compound 1 (*C*) or morphine (*E*) after each treatment were determined by using the tail-flick test. **P* < 0.001 *versus* pretest group. †*P* < 0.01. ‡*P* < 0.001 *versus* posttest (subchronic vehicle) group, two-way ANOVA with appropriate *post hoc* tests. Data in *C* and *E*, n = 6 per group. (*D*, *F*) Quantitative results from *C* and *E* are represented as the area under the curve (AUC). **P* < 0.001 *versus* pretest group. †*P* < 0.01. ‡*P* < 0.001 *versus* posttest (subchronic vehicle), one-way ANOVA with appropriate *post hoc* tests. Data in *D* and *F*, n = 6 to 7 per group. The values indicate the mean ± SD.

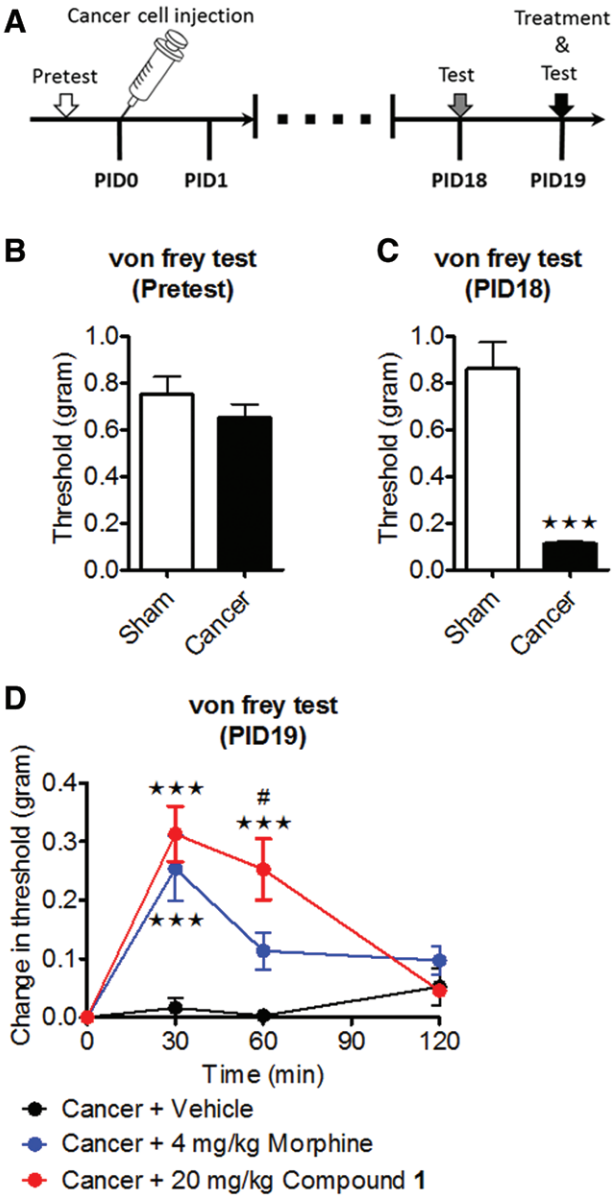

Fig. 7. Effect of morphine and compound 1 on the mechanical allodynia in the cancer-induced pain animal model. (*A*) Flowchart of experiments to determine the effects of morphine or compound 1 on mechanical allodynia. (*B*, *C*) Mice were injected with phosphate-buffered saline (sham) or an intraplantar implantation of mouse B16-F1 melanoma cells to induce tumor growth. Mechanical allodynia with each treatment on postinoculation day (PID) 0 (*B*) or PID 18 (*C*) is presented in grams. **P* < 0.001 *versus* sham-control group, Student's *t* test. Data in *B* and *C* are based on n = 5 per group. (*D*) To test the effect of morphine or compound 1 on cancer-induced pain, mechanical allodynia was evaluated in melanoma cells–implanted mice at the indicated time points (30, 60, and 120 min after drug injection) on PID 19. **P* < 0.001 *versus* vehicle group. †*P* < 0.05 *versus* morphine group, two-way ANOVA with appropriate *post hoc* tests. n = 5 per group. Data are presented as the mean ± SD.

$F_{2,12}$ = 22.6, min $F_{3,36}$ = 78.2, interaction $F_{6,36}$ = 6.3; all P < 0.001; two-way ANOVA). The AUC was 293 ± 15 (min × s) before subchronic morphine treatment and 131 ± 24 (min × s) thereafter (fig. 6D; $F_{2,23}$ = 18.9; P < 0.001; one-way ANOVA). Furthermore, morphine antinociception was also decreased after subchronic treatment with compound 1 as compared to its efficacy before the treatment, indicating that there was no asymmetric cross-tolerance between morphine and compound 1. The magnitude of morphine in time–response curves indicated that there were significant differences between the groups (fig. 6E; treatment $F_{2,12}$ = 377.3, min $F_{3,36}$ = 200.5, interaction $F_{6,36}$ = 49.4; all P < 0.001; two-way ANOVA). The AUC before subchronic morphine treatment was 575 ± 13 (min × s) and 79 ± 29 (min × s) after treatment (fig. 6F; $F_{2,21}$ = 106.3; P < 0.001; one-way ANOVA). Thus, these results indicated that cross-tolerance exists between compound 1 and morphine in mice.

Table 3. Plasma and Brain Concentration Profiles of Compound 1

	Brain Concentration, μg/g	Plasma Concentration, μg/ml
5 min	3.3 ± 0.8	1.6 ± 0.4
60 min	0.2 ± 0.1	0.1 ± 0.1

Samples from the plasma and brain of each mouse were collected at the indicated time points (5 and 60 min) after a single dose of compound 1 (20 mg/kg; intravenously injected). No abnormal clinical observations were found during the experiment. n = 5 per group. The values indicate the mean ± SD.

Compound 1 Relieves Sensory Allodynia Associated with Cancer-induced Pain

Opioids are widely used to manage cancer-related pain. We therefore investigated compound 1 antinociception in a mouse skin cancer pain model (fig. 7A). Sensory allodynia was almost maximal 2 weeks after intraplantar implantation of melanoma cells. The threshold of mechanical allodynia in melanoma cell–implanted mice was decreased significantly on postinoculation day 18 as compared to sham-treated mice (fig. 7B; $P > 0.05$; fig. 7C; $P < 0.001$; Student's t test), and we therefore used this treatment paradigm. Mice were injected with phosphate-buffered saline, compound 1, or morphine on postinoculation day 19 with an equi-antinociceptive dose, and sensory allodynia was measured using the von Frey test to examine the antinociceptive effects of each treatment. Although both compound 1 and morphine exerted similar antinociceptive effects 30 min after treatment, the antinociceptive effect of compound 1 was stronger than that of morphine 60 min after treatment in melanoma cell–implanted mice (fig. 7D; treatment $F_{2,12} = 14$, min $F_{3,36} = 27.2$, interaction $F_{6,36} = 9.5$; all $P < 0.001$; two-way ANOVA). These results suggest that compound 1 produced a better antinociceptive effect than morphine in a model of cancer-induced pain.

Discussion

In this study, we investigated the potential therapeutic benefits and disadvantages of compound 1 as compared to those of morphine. As with morphine, compound 1 demonstrated the highest binding affinity to μ-opioid receptor rather than to δ-opioid receptor or κ-opioid receptor (table 1). Compound 1 acted as a full agonist of all G protein pathways in all μ-opioid, δ-opioid, and κ-opioid receptor–expressing cells (figs. 2A and 3, A and B). However, the antinociceptive effects of both morphine and compound 1 were dependent on μ-opioid receptor activation because only μ-opioid receptor–selective antagonist blocked the effect (fig. 5F), and no antinociceptive effect was induced in μ-opioid receptor knockout mice (fig. 4I). Previous studies have also indicated that δ-opioid receptor activation contributes to opioid tolerance.[19–21] Indeed, antinociceptive tolerance was still induced by subchronic compound 1, although the tolerance to compound 1 developed relatively more slowly than that for morphine (fig. 6A). On the other hand, β-arrestin signaling pathway might be responsible for most of the adverse effects of morphine. Some side effects of morphine, including respiratory depression and tolerance, were diminished in β-arrestin knockout mice,[22,23] and two G-protein–biased ligands, TRV130 and PZM21, which had potent analgesic effects while causing less gastrointestinal dysfunction and respiratory suppression, were discovered.[18,24] Unlike morphine, compound 1 acted as a full agonist of β-arrestin-2 recruitment in μ-opioid and δ-opioid receptor–expressing cells (figs. 2, C and E, and 3C); however, the gastrointestinal motility effects of compound 1 were less pronounced than those of morphine, in both acute and subchronic treatments. This cannot be explained by the previous hypothesis that opioids have fewer side effects when they fail to activate β-arrestin pathways.[22,23] Indeed, β-arrestin-2 plays different roles in small intestine and colon,[25,26] and opioids may activate different μ-opioid receptor isoforms at central and peripheral sites.[27] Furthermore, the inhibition of K^+ and Ca^{2+} channels by opioids also contribute to gut motility.[28,29] Thus, β-arrestin recruitment may not be necessary to generate side effects for all opioids, and molecular mechanisms of compound 1 on gastrointestinal function should be evaluated by further studies in pharmacology, electrophysiology, and molecular biology. On the other hand, the inability of morphine to promote μ-opioid receptor endocytosis has also been implicated in morphine tolerance and withdrawal.[30] These studies led to the adoption of new strategies, including the use of cocktails of opioids designed to promote μ-opioid receptor endocytosis[31,32] or biased to activate G protein pathways rather than β-arrestin pathways[18] to enhance the analgesic effect and diminish side effects. However, recent studies have suggested that endocytosis may not be a dominant consideration in the development of tolerance to every opioid.[33] Compound 1 induced significant μ-opioid receptor endocytosis; however, side effects, including tolerance, remained, although they were less marked than those resulting from morphine treatment (fig. 6). This warrants further investigation of the role of μ-opioid receptor endocytosis in tolerance to compound 1.

Some questions about compound 1–induced antinociception remain. First, in contrast to morphine, which is a full agonist of G protein pathways but only a partial agonist of β-arrestin-2 recruitment and μ-opioid receptor endocytosis, compound 1 is a full agonist of all these μ-opioid receptor signaling pathways. On the other hand, spinal G-protein–coupled inwardly rectifying potassium channel activation plays a critical role in the analgesia evoked by μ-opioid and δ-opioid receptor–selective agonists, including morphine.[34] Compound 1, however, seems to activate G-protein–coupled inwardly rectifying potassium channels only slightly in comparison to morphine, suggesting that non-G-protein–coupled inwardly rectifying

potassium channel activation mechanisms were involved in the analgesic effects of compound 1, much like another opioid, methadone.[35] Furthermore, other opioid receptor–dependent signaling, including the inhibition of calcium influx,[36] phosphorylation of opioid receptors,[37,38] extracellular signal-regulated kinase 1/2,[39] c-Jun N-terminal kinase 2,[40] and signal transducer and activator of transcription 3,[41] still needs to be evaluated to expand the opioid signaling spectrum of compound 1. Second, both morphine and methadone have been reported to regulate antinociception through nonopioid receptors, including the N-methyl-D-aspartic acid receptor,[42] Toll-like receptor 4,[43] and TWIK-1 related K+ channel.[44] It is worth determining whether compound 1 exerts binding affinity to these receptors. A G-protein–coupled receptor profile of compound 1 will also help determine its specificity. Third, as compound 1 markedly accumulated in the brain after 5 min of treatment, it would be interesting to evaluate whether compound 1 crosses the blood–brain barrier through lipid-mediated free diffusion or carrier-mediated transport systems,[45] as well as the effect of compound 1 on *p*-glycoprotein.[46,47] Furthermore, the half-life of compound 1 seems less than 30 min (table 3); however, the antinociception of compound 1 was sustained for at least 3 h (fig. 5C), raising the possibility that active metabolites contributed to the antinociception. The complete pharmacokinetics and metabolic studies should facilitate an understanding of the structure–activity relationship and structure–property relationship of compound 1 and exploring the potential metabolites that are more stable or potent than compound 1. Fourth, the antinociceptive effect of compound 1 in animal models of acute thermal pain hypersensitivity was weaker than that of morphine (fig. 5A–D); however, this is in contrast with the results obtained from the acute mechanical pain hypersensitivity and cancer-induced pain tests (figs. 5E and 7D). It is worth exploring the potential indications for compound 1 in future.

In conclusion, our findings demonstrated that compound 1 acts as a μ-opioid receptor agonist to produce analgesia. Its novel chemical structure provides new insights into opioid-managed pain. Although compound 1 still produces tolerance to analgesia, it causes less constipation than morphine. Further modification of the chemical structure and discovery of the regulatory mechanisms of compound 1 would likely facilitate the discovery of new opioids with fewer adverse effects.

Research Support

Supported by grant Nos. 103-2325-B-400-018, 104-2325-B-400-008, 105-2325-B-400-007, and 101-2311-B-400-005-MY3 obtained from the Ministry of Science and Technology and the Intramural Research Program of the National Health Research Institutes, Zhunan, Miaoli, Taiwan.

Competing Interests

The authors declare no competing interests.

Correspondence

Address correspondence to Dr. Yeh: Institute of Biotechnology and Pharmaceutical Research, National Health Research Institutes, Miaoli 35053, Taiwan. bau9763@nhri.org.tw. Information on purchasing reprints may be found at www.anesthesiology.org or on the masthead page at the beginning of this issue. Anesthesiology's articles are made freely accessible to all readers, for personal use only, 6 months from the cover date of the issue.

References

1. Chou R, Fanciullo GJ, Fine PG, Adler JA, Ballantyne JC, Davies P, Donovan MI, Fishbain DA, Foley KM, Fudin J, Gilson AM, Kelter A, Mauskop A, O'Connor PG, Passik SD, Pasternak GW, Portenoy RK, Rich BA, Roberts RG, Todd KH, Miaskowski C; American Pain Society-American Academy of Pain Medicine Opioids Guidelines Panel: Clinical guidelines for the use of chronic opioid therapy in chronic noncancer pain. J Pain 2009; 10:113–30
2. Dai F, Silverman DG, Chelly JE, Li J, Belfer I, Qin L: Integration of pain score and morphine consumption in analgesic clinical studies. J Pain 2013; 14:767–77.e8
3. Tao R, Auerbach SB: Opioid receptor subtypes differentially modulate serotonin efflux in the rat central nervous system. J Pharmacol Exp Ther 2002; 303:549–56
4. Chen Y, Mestek A, Liu J, Hurley JA, Yu L: Molecular cloning and functional expression of a mu-opioid receptor from rat brain. Mol Pharmacol 1993; 44:8–12
5. Loh HH, Liu HC, Cavalli A, Yang W, Chen YF, Wei LN: mu Opioid receptor knockout in mice: Effects on ligand-induced analgesia and morphine lethality. Brain Res Mol Brain Res 1998; 54:321–6
6. Zacny J, Bigelow G, Compton P, Foley K, Iguchi M, Sannerud C: College on Problems of Drug Dependence taskforce on prescription opioid non-medical use and abuse: Position statement. Drug Alcohol Depend 2003; 69:215–32
7. Compton WM, Volkow ND: Major increases in opioid analgesic abuse in the United States: Concerns and strategies. Drug Alcohol Depend 2006; 81:103–7
8. Gilson AM, Ryan KM, Joranson DE, Dahl JL: A reassessment of trends in the medical use and abuse of opioid analgesics and implications for diversion control: 1997-2002. J Pain Symptom Manage 2004; 28:176–88
9. Tao PL, Law PY, Loh HH: Search for the "ideal analgesic" in pain treatment by engineering the mu-opioid receptor. IUBMB Life 2010; 62:103–11
10. Cheng MF, Ou LC, Chen SC, Chang WT, Law PY, Loh HH, Chao YS, Shih C, Yeh SH, Ueng SH: Discovery, structure-activity relationship studies, and anti-nociceptive effects of 1-phenyl-3,6,6-trimethyl-1,5,6,7-tetrahydro-4H-indazol-4-one as novel opioid receptor agonists. Bioorg Med Chem 2014; 22:4694–703
11. Lee PT, Chao PK, Ou LC, Chuang JY, Lin YC, Chen SC, Chang HF, Law PY, Loh HH, Chao YS, Su TP, Yeh SH: Morphine drives internal ribosome entry site-mediated hnRNP K translation in neurons through opioid receptor-dependent signaling. Nucleic Acids Res 2014; 42:13012–25
12. Huang SP, Chien JY, Tsai RK: Ethambutol induces impaired autophagic flux and apoptosis in the rat retina. Dis Model Mech 2015; 8:977–87
13. Mathews JL, Smrcka AV, Bidlack JM: A novel Gbetagamma-subunit inhibitor selectively modulates mu-opioid-dependent antinociception and attenuates acute morphine-induced antinociceptive tolerance and dependence. J Neurosci 2008; 28:12183–9
14. Cao YQ, Mantyh PW, Carlson EJ, Gillespie AM, Epstein CJ, Basbaum AI: Primary afferent tachykinins are required to experience moderate to intense pain. Nature 1998; 392:390–4

15. Chaplan SR, Bach FW, Pogrel JW, Chung JM, Yaksh TL: Quantitative assessment of tactile allodynia in the rat paw. J Neurosci Methods 1994; 53:55–63
16. Lüscher C, Slesinger PA: Emerging roles for G protein-gated inwardly rectifying potassium (GIRK) channels in health and disease. Nat Rev Neurosci 2010; 11:301–15
17. Kuzhikandathil EV, Yu W, Oxford GS: Human dopamine D3 and D2L receptors couple to inward rectifier potassium channels in mammalian cell lines. Mol Cell Neurosci 1998; 12:390–402
18. DeWire SM, Yamashita DS, Rominger DH, Liu G, Cowan CL, Graczyk TM, Chen XT, Pitis PM, Gotchev D, Yuan C, Koblish M, Lark MW, Violin JD: A G protein-biased ligand at the μ-opioid receptor is potently analgesic with reduced gastrointestinal and respiratory dysfunction compared with morphine. J Pharmacol Exp Ther 2013; 344:708–17
19. Kest B, Lee CE, McLemore GL, Inturrisi CE: An antisense oligodeoxynucleotide to the delta opioid receptor (DOR-1) inhibits morphine tolerance and acute dependence in mice. Brain Res Bull 1996; 39:185–8
20. Zhu Y, King MA, Schuller AG, Nitsche JF, Reidl M, Elde RP, Unterwald E, Pasternak GW, Pintar JE: Retention of supraspinal delta-like analgesia and loss of morphine tolerance in delta opioid receptor knockout mice. Neuron 1999; 24:243–52
21. Shippenberg TS, Chefer VI, Thompson AC: Delta-opioid receptor antagonists prevent sensitization to the conditioned rewarding effects of morphine. Biol Psychiatry 2009; 65:169–74
22. Bohn LM, Lefkowitz RJ, Gainetdinov RR, Peppel K, Caron MG, Lin FT: Enhanced morphine analgesia in mice lacking beta-arrestin 2. Science 1999; 286:2495–8
23. Raehal KM, Walker JK, Bohn LM: Morphine side effects in beta-arrestin 2 knockout mice. J Pharmacol Exp Ther 2005; 314:1195–201
24. Manglik A, Lin H, Aryal DK, McCorvy JD, Dengler D, Corder G, Levit A, Kling RC, Bernat V, Hübner H, Huang XP, Sassano MF, Giguère PM, Löber S, Da Duan, Scherrer G, Kobilka BK, Gmeiner P, Roth BL, Shoichet BK: Structure-based discovery of opioid analgesics with reduced side effects. Nature 2016; 537:185–90
25. Ross GR, Gabra BH, Dewey WL, Akbarali HI: Morphine tolerance in the mouse ileum and colon. J Pharmacol Exp Ther 2008; 327:561–72
26. Kang M, Maguma HT, Smith TH, Ross GR, Dewey WL, Akbarali HI: The role of β-arrestin2 in the mechanism of morphine tolerance in the mouse and guinea pig gastrointestinal tract. J Pharmacol Exp Ther 2012; 340:567–76
27. Mori T, Shibasaki Y, Matsumoto K, Shibasaki M, Hasegawa M, Wang E, Masukawa D, Yoshizawa K, Horie S, Suzuki T: Mechanisms that underlie μ-opioid receptor agonist-induced constipation: Differential involvement of μ-opioid receptor sites and responsible regions. J Pharmacol Exp Ther 2013; 347:91–9
28. Cherubini E, North RA: Mu and kappa opioids inhibit transmitter release by different mechanisms. Proc Natl Acad Sci USA 1985; 82:1860–3
29. Tokimasa T, Morita K, North A: Opiates and clonidine prolong calcium-dependent after-hyperpolarizations. Nature 1981; 294:162–3
30. Kim JA, Bartlett S, He L, Nielsen CK, Chang AM, Kharazia V, Waldhoer M, Ou CJ, Taylor S, Ferwerda M, Cado D, Whistler JL: Morphine-induced receptor endocytosis in a novel knockin mouse reduces tolerance and dependence. Curr Biol 2008; 18:129–35
31. He L, Fong J, von Zastrow M, Whistler JL: Regulation of opioid receptor trafficking and morphine tolerance by receptor oligomerization. Cell 2002; 108:271–82
32. He L, Whistler JL: An opiate cocktail that reduces morphine tolerance and dependence. Curr Biol 2005; 15:1028–33
33. Dang VC, Christie MJ: Mechanisms of rapid opioid receptor desensitization, resensitization and tolerance in brain neurons. Br J Pharmacol 2012; 165:1704–16
34. Marker CL, Luján R, Loh HH, Wickman K: Spinal G-protein-gated potassium channels contribute in a dose-dependent manner to the analgesic effect of mu- and delta- but not kappa-opioids. J Neurosci 2005; 25:3551–9
35. Rodriguez-Martin I, Braksator E, Bailey CP, Goodchild S, Marrion NV, Kelly E, Henderson G: Methadone: Does it really have low efficacy at micro-opioid receptors? Neuroreport 2008; 19:589–93
36. Rusin KI, Giovannucci DR, Stuenkel EL, Moises HC: Kappa-opioid receptor activation modulates Ca2+ currents and secretion in isolated neuroendocrine nerve terminals. J Neurosci 1997; 17:6565–74
37. El Kouhen R, Kouhen OM, Law PY, Loh HH: The absence of a direct correlation between the loss of [D-Ala2, MePhe4,Gly5-ol]enkephalin inhibition of adenylyl cyclase activity and agonist-induced mu-opioid receptor phosphorylation. J Biol Chem 1999; 274:9207–15
38. Schulz S, Mayer D, Pfeiffer M, Stumm R, Koch T, Höllt V: Morphine induces terminal micro-opioid receptor desensitization by sustained phosphorylation of serine-375. EMBO J 2004; 23:3282–9
39. Macey TA, Lowe JD, Chavkin C: Mu opioid receptor activation of ERK1/2 is GRK3 and arrestin dependent in striatal neurons. J Biol Chem 2006; 281:34515–24
40. Tan M, Walwyn WM, Evans CJ, Xie CW: p38 MAPK and beta-arrestin 2 mediate functional interactions between endogenous micro-opioid and alpha2A-adrenergic receptors in neurons. J Biol Chem 2009; 284:6270–81
41. Goldsmith JR, Uronis JM, Jobin C: Mu opioid signaling protects against acute murine intestinal injury in a manner involving Stat3 signaling. Am J Pathol 2011; 179:673–83
42. Ebert B, Andersen S, Krogsgaard-Larsen P: Ketobemidone, methadone and pethidine are non-competitive N-methyl-D-aspartate (NMDA) antagonists in the rat cortex and spinal cord. Neurosci Lett 1995; 187:165–8
43. Wang X, Loram LC, Ramos K, de Jesus AJ, Thomas J, Cheng K, Reddy A, Somogyi AA, Hutchinson MR, Watkins LR, Yin H: Morphine activates neuroinflammation in a manner parallel to endotoxin. Proc Natl Acad Sci USA 2012; 109:6325–30
44. Devilliers M, Busserolles J, Lolignier S, Deval E, Pereira V, Alloui A, Christin M, Mazet B, Delmas P, Noel J, Lazdunski M, Eschalier A: Activation of TREK-1 by morphine results in analgesia without adverse side effects. Nat Commun 2013; 4:2941
45. Pardridge WM: Drug transport across the blood-brain barrier. J Cereb Blood Flow Metab 2012; 32:1959–72
46. Choudhuri S, Klaassen CD: Structure, function, expression, genomic organization, and single nucleotide polymorphisms of human ABCB1 (MDR1), ABCC (MRP), and ABCG2 (BCRP) efflux transporters. Int J Toxicol 2006; 25:231–59
47. Sakaeda T, Nakamura T, Okumura K: MDR1 genotype-related pharmacokinetics and pharmacodynamics. Biol Pharm Bull 2002; 25:1391–400